Preliminary Study on Effects of Neck Exoskeleton Structural Design in Patients With Amyotrophic Lateral Sclerosis

David Demaree, Joseph Brignone, Mark Bromberg, and Haohan Zhang, *Member, IEEE*

***Abstract*— Neck muscle weakness due to amyotrophic lateral sclerosis (ALS) can result in dropped head syndrome, adversely impacting the quality of life of those affected. Static neck collars are currently prescribed to hold the head in a fixed upright position. However, these braces are uncomfortable and do not allow any voluntary head-neck movements. By contrast, powered neck exoskeletons have the potential to enable head-neck movements. Our group has recently improved the mechanical structure of a state-of-the-art neck exoskeleton through a weighted optimization. To evaluate the effect of the structural changes, we conducted an experiment in which patients with ALS were asked to perform head-neck tracking tasks while using the two versions of the neck exoskeleton. We found that the neck muscle activation was significantly reduced when assisted by the structurally enhanced design compared to no assistance provided. The improved structure also improved kinematics tracking performance, allowing users to better achieve the desired head poses. In comparison, the previous design did not help reduce the muscle effort required to perform these tasks and even slightly worsened the kinematic tracking performance. It was also found that biomechanical benefits gained from using the structurally improved design were consistent across participants with both mild and severe neck weakness. Furthermore, we observed that participants preferred to use the powered neck exoskeletons to voluntarily move their heads and make eye contact during a conversation task rather than remain in a fixed upright position. Each of these findings highlights the importance of the structural design of neck exoskeletons in achieving desired biomechanical benefits and suggests that neck exoskeletons can be a viable method to improve the daily life of patients with ALS.**

***Index Terms*— Powered neck exoskeleton, dropped head syndrome, physical human-robot interaction, amyotrophic lateral sclerosis.**

I. Introduction

AMYOTROPHIC lateral sclerosis (ALS), a fatal neurodegenerative disease, causes loss of motor neurons leading to progressive and systemic muscle weakness. Neck muscle weakness is common, resulting in difficulty maintaining an upright head posture for an extended time due to fatigue ("dropped head syndrome"). In the most severe form ($\sim$3% of ALS patients [1]), the head completely drops, leading to a "chin-on-chest posture". The resulting prolonged neck flexion causes bending in the airway of an individual, exacerbating respiratory difficulties that ALS patients already experience [2]. The prolonged chin-on-chest posture also leads to neck pain, spinal deformity, and poor overall posture due to compensation in the thoracolumbar and pelvic segments to help maintain a horizontal gaze for safe ambulation [3]. Finally, ALS patients with dropped head syndrome are susceptible to social isolation due to difficulty maintaining eye contact and performing common gestures (e.g., nodding) [4].

Clinical options to treat dropped head syndrome are limited. Static neck collars are primarily prescribed [5]; however, current collars support the head at the chin, making it even more challenging to speak, swallow, and breathe [6]. These collars by design immobilize the head, leading to discomfort and further limiting social interactions [7]. As a result, few patients with ALS use their prescribed neck collars at home; many patients prefer alternative strategies like using travel pillows or resting their heads on a reclining wheelchair [8]. To date, the only alternative neck collar was developed at the University of Sheffield [9]. This device sits on a user's chest and supports the head at the chin using customized flexible beams that provide support while also allowing the user to voluntarily move their head around the upright pose. However, a recent study in patients with ALS revealed this alternative neck collar provides no significant perceivable benefit over traditional

Manuscript received 15 November 2023; revised 14 March 2024; accepted 2 May 2024. Date of publication 6 May 2024; date of current version 10 May 2024. This work was supported in part by the National Science Foundation under Grant 2240508. *(Corresponding author: Haohan Zhang.)*

This work involved human subjects or animals in its research. Approval of all ethical and experimental procedures and protocols was granted by The University of Utah under Application No. 00145893.

David Demaree and Joseph Brignone are with the Department of Mechanical Engineering, The University of Utah, Salt Lake City, UT 84112 USA (e-mail: david.demaree@utah.edu; joseph.brignone@utah.edu).

Mark Bromberg is with the Department of Neurology, The University of Utah, Salt Lake City, UT 84112 USA (e-mail: mark.bromberg@hsc.utah.edu).

Haohan Zhang is with Utah Wearable Robotics Laboratory, Salt Lake City, UT 84112 USA, and also with the Department of Mechanical Engineering and the Robotics Center, The University of Utah, Salt Lake City, UT 84112 USA (e-mail: haohan.zhang@utah.edu).

This article has supplementary downloadable material available at https://doi.org/10.1109/TNSRE.2024.3397584, provided by the authors.

Digital Object Identifier 10.1109/TNSRE.2024.3397584

static collars [10]. Furthermore, patients with severe dropped head syndrome, which is imminent due to the progressive nature of ALS, do not have the necessary strength to initiate the subtle head-neck motions that this collar allows [11]. Therefore, there is a critical unmet need to better support and actively enable head-neck motions to treat dropped head syndrome in ALS and improve the physical and emotional well-being of patients with ALS.

To address this need, Zhang and Agrawal at Columbia University previously pioneered a powered neck exoskeleton [12]. This device (*Columbia Exo*) has 3 degrees-of-freedom (DoF) and features a novel parallel linkage design that couples translational and rotational movement to best match the observed natural dynamic head-neck motions in healthy participants. For the first time, a user can perform spatial head rotations up to 70% head-neck range of motion with assistance provided by a robotic neck device [13]. Recent studies demonstrated that the *Columbia Exo* can empower ALS patients with mild dropped head syndrome to perform large ranges of head rotations [14] and reduce their neck muscular effort (estimated by using surface electromyography (EMG) [15], [16]) when following target head trajectories with exoskeleton assistance [17].

Despite these impressive achievements, however, it has been shown that the head can be easily perturbed from a desired pose by the gravitational moment of the head even when the actuators of this exoskeleton are locked in place [18]. This is problematic, as the *Columbia Exo* may not be able to maintain the head at desired poses for users with severe neck weakness. In the previous patient evaluation [17], the head kinematics were computed by using the motor angles of the exoskeleton, which is limited because it does not account for errors caused by its structural deficiencies. Because there was no independent kinematic measurement as a ground truth, it is unclear whether the observed EMG reduction of ALS participants was due to the assistance from the *Columbia Exo* or simply caused by reduced motion of the head. Furthermore, we do not yet know how the neck exoskeleton was perceived by the users or how improved head-neck movements can benefit their daily activities. Addressing these remaining questions is important because it will provide critical insights into technology development to ultimately provide clinically available neck exoskeletons to patients with neck weakness.

Our group at the University of Utah has recently developed a new powered neck exoskeleton (*Utah Exo*) which was based on the *Columbia Exo* but features an enhanced mechanical structure [18]. Specifically, the *Utah Exo* was optimized to efficiently transmit torques from the motors to the head through a weighted optimization. The mechanical joints and linkages were also redesigned to reduce deflection and joint play. As a result, the *Utah Exo* is more mechanically stable than its predecessor during bench tests [18].

We expected that these mechanical improvements would translate into greater biomechanical benefits: more accurate head positioning and lower muscular efforts measured by EMG, in patients with ALS. We also postulated that these benefits would be retained in patients with severe neck muscle weakness, which would be a significant improvement over the previous system that was only effective for patients with mild neck weakness. We conducted an experiment to evaluate the performance of the *Utah Exo* in patients with ALS, as compared to the state-of-the-art *Columbia Exo*. We show that the greater structural stability of the *Utah Exo* further reduced the neck muscle activation and achieved more accurate tracking kinematics. We also show that these biomechanical observations remained for patients with severe neck muscle weakness using the *Utah Exo* but not the *Columbia Exo*. These results highlight the importance of the structural design of neck exoskeletons and serve as a significant step towards using the neck exoskeleton technology to restore head-neck mobility in patients with ALS.

II. Methods

In this section, we will first provide the necessary engineering background of the neck exoskeleton design and control methods, followed by descriptions of the user study design and data analyses.

A. Design and Control of the Neck Exoskeletons

Both neck exoskeletons (i.e., *Utah Exo* and *Columbia Exo*) in this study adopted an identical parallel mechanism in their design. In this mechanism, three chains of linkages, joined by revolute, revolute, and spherical joints (3-RRS), were used to connect the shoulder and head attachments of the exoskeleton. The revolute joint axes within each chain intersect at a point that is stationary relative to the shoulder attachment. These kinematic constraints result in the mechanism that has three degrees-of-freedom, with coupled rotation and translation of the head attachment. The rotation-translation coupling was previously optimized based on head-neck kinematics observed from healthy individuals [13]. The moment applied on the headband $\boldsymbol{m}$ can be related to the motor torques $\boldsymbol{\tau}$ by,

$$\boldsymbol{m} = \boldsymbol{J}\boldsymbol{\tau}\,, \tag{1}$$

where $\boldsymbol{J}$ is a 3×3 Jacobian matrix that depends on the configuration and geometry of the exoskeleton [19], [20]. An ill-conditioned Jacobian matrix indicates that the exoskeleton is near its singularity configuration [21], which means that actuator torques are not efficiently transmitted to the end effector. As a result, large actuator torques are required to counterbalance relatively small moments applied to the head. In other words, the end-effector can be easily perturbed by the external load despite sufficiently high actuator torques (e.g., locked in place).

In contrast with the *Columbia Exo* (Fig. 1A) which prioritized the range of motion of the exoskeleton, we added a term to the objective function for the design optimization of the *Utah Exo* (Fig. 1B) which prioritized the condition number of the Jacobian matrix at the exoskeleton home configuration. Specifically, the objective function was formulated as a weighted sum of the two competing objectives: $c = w_1 g_1 + w_2 g_2$, where g_1 is the normalized range of motion in two anatomical planes (sagittal and frontal planes) where the full range in each plane is 180°, g_2 is the reciprocal of the condition number of the Jacobian matrix at the upright neutral pose, and $w_1 = 0.35$ and $w_2 = 0.65$ are hand-selected weights

TABLE I
PARTICIPANT CHARACTERISTICS

Participant ID	Sex	Age (yrs)	ALSFRS-r [1]	%FVC [2]	Self-reported Neck Weakness	Use a Wheelchair	Had Residual Hand Function
001	M	35	7	20	Yes	Yes	Yes
002	M	62	38	56	No	Yes	Yes
003	M	55	30	61	Yes	No	Yes
004	F	72	15	39	Yes	Yes	No
005	M	51	26	40	No	No	Yes
006	M	64	39	78	No	Yes	Yes

[1] ALS functional rating scale (revised), A higher score indicates a higher functional ability during daily activities (e.g., dressing). A full score is 48.
[2] Percentage forced vital capacity, normalized with respect to the forced vital capacity measured at first admission.

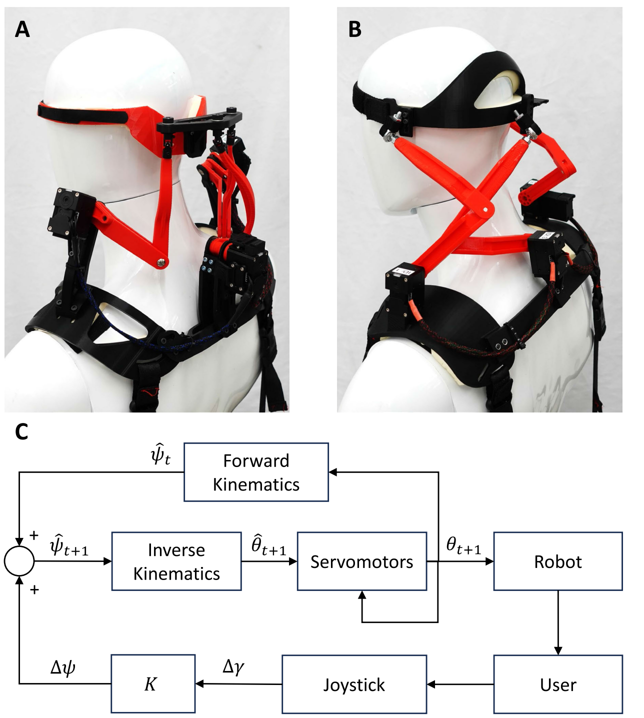

Fig. 1. **Neck exoskeletons used in this study.** (A) *Columbia Exo*. (B) *Utah Exo*. We intentionally fabricated both exoskeletons to have a similar appearance to eliminate potential bias. (C) Control scheme of the joystick interface used in this study.

TABLE II
MOVEMENT TASKS SELECTED FOR THE EXPERIMENT

Tasks	Target Head Trajectories [°]
upright	$\boldsymbol{\psi}(t) = \mathbf{0}$
flexion-extension	$\psi_x(t) = 15 \sin 1.124\, t - 5$
axial rotation	$\psi_z(t) = 15 \sin 0.845\, t$
flexion pose	$\psi_x(t) = \begin{cases} -6.67\, t & 0 \leq t < 3 \\ -20 & 3 \leq t \leq 27 \\ 6.67\, t - 200 & 27 < t \leq 30 \end{cases}$
left rotation pose	$\psi_z(t) = \begin{cases} 6.67\, t & 0 \leq t < 3 \\ 20 & 3 \leq t \leq 27 \\ -6.67\, t + 200 & 27 < t \leq 30 \end{cases}$
right rotation pose	$\psi_z(t) = \begin{cases} -6.67\, t & 0 \leq t < 3 \\ -20 & 3 \leq t \leq 27 \\ 6.67\, t - 200 & 27 < t \leq 30 \end{cases}$

for the two objectives. As a result, the objective c ranges between 0 and 1. Additional constraints were used in the optimization including symmetry constraint about the sagittal plane as well as the ranges for the geometric parameters to avoid interference with the user. A genetic algorithm was used, in which design candidates were encoded as an array of numbers to find a globally optimal design that provides the highest composite score (between 0 and 1) based on the weighted objective function. We also upgraded the linkages and joints in the *Utah Exo* to reduce the deflection of the mechanical components and play within the joints. The spherical joint, previously implemented via a plastic universal joint in series with a revolute joint, was replaced with precise metal ball-socket joint in each chain. The middle revolute joints using low-profile bushing and binding posts were upgraded using press-fit ball bearings and a machined shaft. As a result, the *Utah Exo* is far more resilient to external perturbations in bench experiments [18]. In this study, the two exoskeletons were fabricated with similar appearances to remove any biases from the participants, as shown in Fig. 1.

To control the neck exoskeleton movement, a position controller was adopted (Fig. 1C). The inverse kinematics model of the exoskeleton [13] was used to generate the trajectories $\boldsymbol{\theta}$ of the servomotors based on the target head orientation $\boldsymbol{\psi}$. When the exoskeleton was controlled to prescribe motion to the head, the target head orientation was generated based on the target avatar motion trajectories (Table II). When the participant self-controlled the exoskeleton movement using a joystick, this target head orientation was acquired based on the current head orientation, estimated using the forward kinematics model of the robot, and the joystick angle input by the participant. The joystick angle corresponds to an angular increment of the head orientation, which was modulated by a controller gain K. This controller gain was hand-tuned based on the preference of each participant. The joystick has two degrees of freedom: forward/backward motion maps to flexion/extension, and lateral motion maps to axial rotation of the head. A customized joystick was used whose handle was designed so that it can be easily grasped by ALS patients who often have reduced hand functions.

B. Participants

Six individuals diagnosed with ALS were enrolled in this study (Table I). All participants were treated and referred by the Motor Neuron Disease clinic at the University of Utah Hospital. The Institutional Review Board at the University of Utah approved this study (IRB #00145893). Signed informed consent was obtained prior to any data collection. Of the six participants, three have self-reported neck weakness and/or use a neck collar during their daily activities.

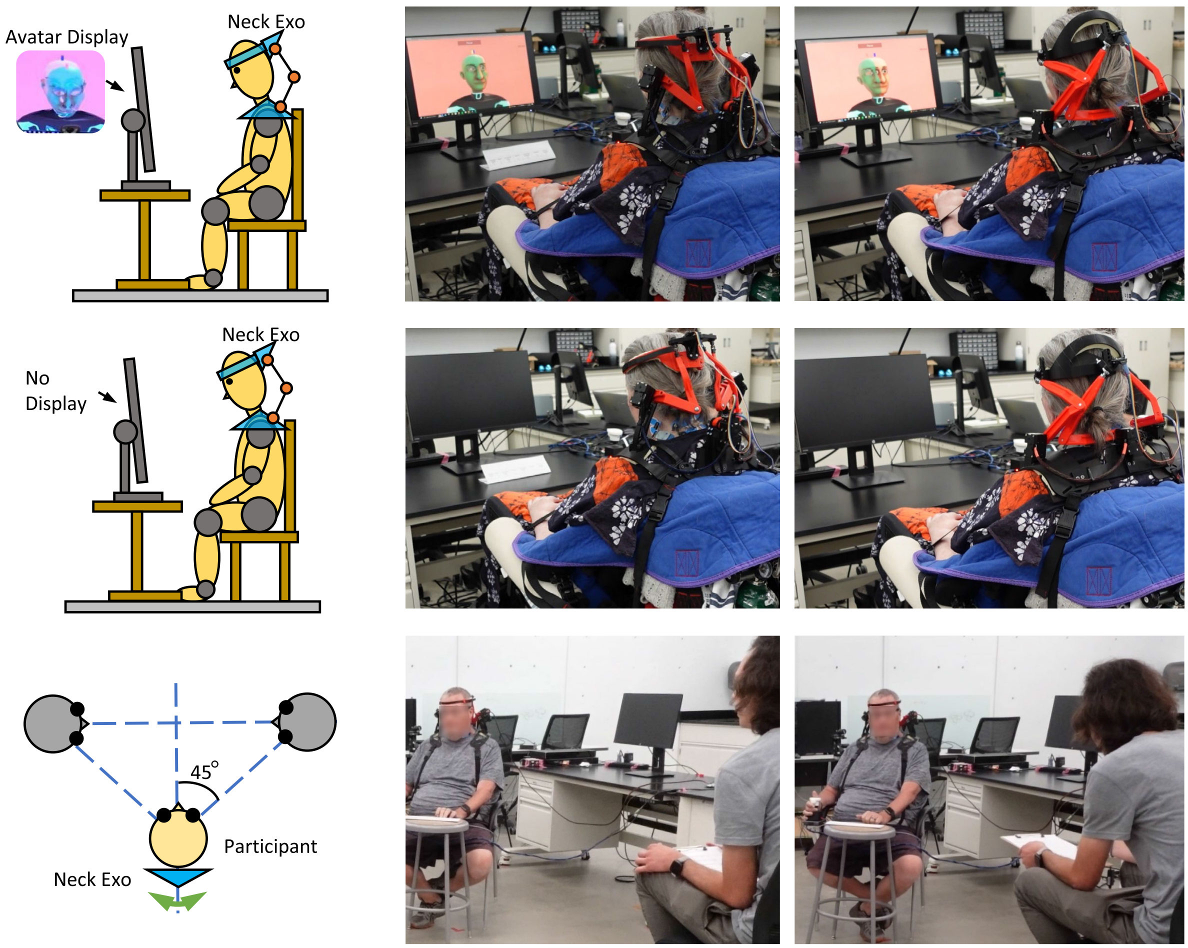

Fig. 2. **Experimental protocol.** (Top row, left to right) A schematic of the *visual* condition; a participant using the *Columbia Exo* to follow the on-screen avatar motion; and the same participant using the *Utah Exo* to follow the same motion. (Middle row, left to right) A schematic of the *no visual* condition; a participant relying on the *Columbia Exo* to move her head; the same participant relying on the *Utah Exo* to move her head according to a target trajectory. (Bottom, left to right) A schematic of the conversation task; a participant converses with the experimenters with the head fixed by the exoskeleton; the same participant controls the neck exoskeleton through a joystick to make eye contact with the experimenters.

C. Protocol

During a single visit, each participant was seated in front of a computer screen and the height of the screen was adjusted based on the preference of the participant. Wheelchair users remained in their wheelchairs while others used a stationary chair throughout the experiment. Surface EMG sensors (DTS, Noraxon, AZ, USA) were then placed on the target muscles by trained personnel. Four neck muscles were monitored: left and right sternocleidomastoid (SCM) and splenius capitis (SC) muscles. Two inertial measurement units (IMU, BNO055, Bosch Sensortec, CA, USA) were placed on the shoulder pads and the headbands, respectively, to measure the head rotations with respect to the shoulders. The IMU sensors were calibrated with the head of the participant at their upright neutral pose. Because each trial starts from the upright neutral pose, the IMU sensors were automatically recalibrated at the beginning of the trial to mitigate sensor drift.

A randomized crossover design was used. Each participant used both exoskeleton devices on the same day. A balanced randomization was performed to assign the order of using the devices to each participant. While using each device, the participant was asked to perform tasks in three conditions: 1) follow the on-screen target motion under their own power (Baseline condition); 2) follow the on-screen target motion with prescribed assistance from an exoskeleton device (Visual condition, Fig. 2, Top); and 3) stay relaxed and allow the device to move their head through prescribed motion without any visual feedback (No-visual condition, Fig. 2, Middle). Using each device, the participant always started with the Baseline condition. The order of Visual and No-visual conditions was randomized among the participants (unbalanced).

During the Baseline and Visual conditions, the visual feedback was provided through an avatar interface [22], [23]. On this interface, two avatars were overlaid: one with solid colors was used to provide motion instructions ("target avatar") and the other with translucent colors was used to reflect the actual head-neck motions of the participant, measured by the IMU sensors. In addition to using the 3D facial features of the avatars to follow the prescribed motions, an indicator was placed on top of the avatar's head where the color of the indicator was used to provide extra information about the tracking error to the participant (i.e., green$< 3°$, yellow $3° \sim 8°$, and red $> 8°$ error). In each condition, six-movement tasks (Table II) were performed: 1) maintaining an upright posture (*upright*) for 30 seconds, 2) following a dynamic motion in the sagittal plane (*flexion-extension*) for six cycles, 3) following a dynamic motion in the horizontal plane for six cycles (*axial rotation*), 4) maintaining a 30° flexion head pose (*flexion pose*) for 30 seconds, 5) maintaining a 20° left rotation pose for 30 seconds (*left rotation pose*), and 6) maintaining a 20° right rotation pose for 30 seconds (*right rotation pose*).

After completing movement tasks using each device, we used a questionnaire to collect the user's qualitative opinions regarding the device in 12 different domains (Table IV). The participant gave their answer to each question on a 7-point Likert scale. Of the six participants, five had remaining hand functions (Table I) to use the joystick to control the neck exoskeletons. The speed of the joystick was chosen by each participant. For these five participants, we designed a conversation task while asking the questionnaire questions (Fig. 2, Bottom): two experimenters sat 90 degrees apart from the participant and alternated asking the questions. For the first six questions, the head of the participant was held upright by the exoskeleton, intended to simulate conducting a conversation while wearing a static neck collar. For the remaining six questions, the participant was given the choice to use a joystick to control the exoskeleton to move their head. In addition to using the questionnaire, open-ended comments were also collected from the participants. For the one participant who could not use the joystick, the same questions were asked regarding each device, although the head was not supported by the neck exoskeletons during the interview. The interview session took roughly 10 minutes to complete. The overall length of the experiment was ~2 hours. Short breaks were provided between trials and as requested by participants.

D. Data Processing

All data was processed using MATLAB (2023b, Mathworks, Natick, MA). Using the Euler angles recorded by the two IMU sensors, the head and trunk orientations were described in rotation matrices. The head angles relative to the trunk were then calculated based on these rotation matrices and expressed in fixed x-y-z Euler sequence. The mean absolute error (difference between the target and actual head angles) of each trial was computed and the maximum among three head angles was used to quantify the *Error* (kinematic outcome variable) for each trial, i.e.,

$$Error = max(\overline{|\boldsymbol{\psi}_t - \boldsymbol{\psi}_a|}), \tag{2}$$

where $\boldsymbol{\psi}_t$ and $\boldsymbol{\psi}_a$ are 3×1 vectors representing the target and actual head angles.

DC offset of the raw EMG signals was first removed, followed by bandpass-filtering (20~450 Hz) and a full-wave rectification. A moving average approach was then used (window size 100 ms) to obtain the profile of the EMG data. Lastly, the processed EMG signal of each muscle was normalized with respect to the highest value of the raw EMG of that muscle during the two baseline trials of each participant. The mean of the normalized EMG was calculated for each muscle and the average of the mean (*Average EMG*) was used as the EMG outcome variable for each trial.

E. Statistics

The response variables are the *Error* and *Average EMG*. We first established that both response variables from the two Baseline conditions were not significantly different using paired Wilcoxon signed-rank test ($\alpha = 0.05$). We then considered the factors in this study as *Device* and *Movement*. The *Device* includes the *Columbia Exo*, *Utah Exo*, and *No Assistance* (mean of the two Baseline conditions) groups; and the *Movement* includes *upright*, *flexion/extension*, *axial rotation*, *flexion pose*, *left rotation pose*, and *right rotation pose* groups.

Two-factorial Analysis of variance (ANOVA) was used to determine the effect of factors on *Average EMG*. The interaction effects between factors were included. Normality assumption for ANOVA was verified using the Shapiro-Wilk test for each ANOVA model. Alternatively, the Friedman test was used to determine the main effect of *Device*, with the secondary factor being *Movement*, on *Error* because the normality requirement for ANOVA was not met. Interaction effects were therefore not examined in this scenario. These tests were performed for each visual condition (i.e., Visual and No-visual) separately, and were first conducted on data from all participants and then on only participants with self-reported weakness (see Table I). The unadjusted significance level α was 0.05. Post-hoc multiple comparison tests and paired Wilcoxon signed-rank tests were performed as appropriate, with adjusted significance value using the Dunn-Sidak correction method.

For questionnaire responses, numerical values were assigned to the user responses using 7-point Likert scales. For each question (12 questions total), pairwise comparisons were performed using Wilcoxon signed-rank tests ($\alpha = 0.05$).

III. Results

A. Representative Data

Fig. 3 shows the representative data from one participant with self-reported neck weakness. In this example, the target head motion is a dynamic neck flexion-extension in the sagittal plane. The motion was shown to the participant using the on-screen avatars. During baselines when no assistance were provided by the robot, on average, the participant had relatively large tracking errors. This is also reflected in their EMG data where no clear pattern was identified: the neck muscles, both extensors (SC) and flexors (SCM), fired constantly throughout the motion task. By contrast, when the motion was assisted by either neck exoskeleton, the tracking performance improved in the sagittal plane (i.e., pitch angle). The out-of-plane tracking (i.e., Roll and Yaw) was better and more consistent when assisted by the *Utah Exo* than by the *Columbia Exo*. When assisted by either exoskeleton, the EMG is decreased in each muscle during each motion cycle, and the reduction is more profound when using the *Utah Exo*.

B. Group Results

Participants were asked to perform tasks first under their own power while using either device (Baseline condition). The order of using either device was randomized. Between

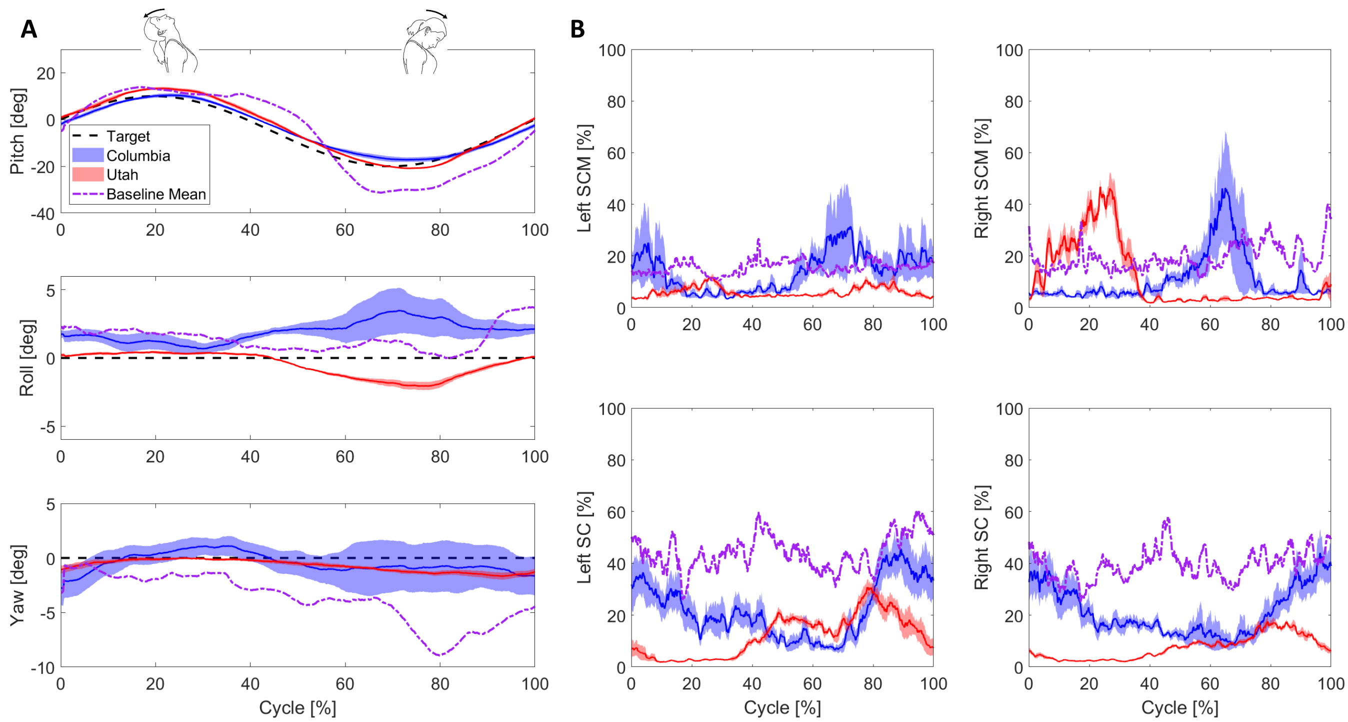

Fig. 3. **Representative data from one participant with self-reported weakness when visual feedback was provided.** (A) Head angular trajectories (pitch, roll, and yaw) while tracking a dynamic flexion/extension movement. The kinematics are segmented based on cycles where the solid lines are the means, and the bands are the standard errors of the repetitions. The target trajectories and the mean of the baselines (when tracking with visual feedback but without exoskeleton assistance) are shown in dashed black and dot-dashed purple lines. The head angles are represented in degrees using fixed x-y-z sequence. (B) EMG of four neck muscles (left/right SCM and SC) of the same participant during the same flexion/extension task. The EMG are filtered, normalized, and segmented based on the kinematic data. Solid lines are the means, and the bands are the standard errors of the repetitions. The mean of the two baselines are shown in dot-dashed purple lines.

TABLE III
STATISTICAL TESTING RESULTS. ASTERISKS INDICATE RESULTS THAT ARE SIGNIFICANT

		Visual		No Visual	
		Avg. EMG	*Error*	*Avg. EMG*	*Error*
All	*Device*	**0.0025***	**<0.0001***	**0.0002***	**0.0023***
	Movement	0.0641	n/a	0.0636	n/a
	Interaction	0.8623	n/a	0.9554	n/a
Weak	*Device*	0.0758	**0.0026***	**0.0064***	0.5488
	Movement	0.0863	n/a	0.3242	n/a
	Interaction	0.9935	n/a	0.9946	n/a

these two baselines, we found that the neck muscle activation (*Average EMG*) was not significantly different among all participants or among only weak participants ($p = 0.0758$ and $p = 0.6475$, respectively). Similarly, the tracking performance (*Error*) was not significantly different either among all participants or among only weak participants ($p = 0.4508$ and $p = 0.4204$, respectively). Therefore, we can conclude that participants performed the tasks similarly during the baseline sessions. The remaining results present the average of data recorded from the two baselines (i.e., *No Assistance* group). Using the average of the baseline data reduces the number of multiple comparisons and preserves the power of our analysis.

When the visual feedback was provided, the means of *Average EMG* among three *Device* groups (i.e., *Columbia Exo*, *Utah Exo*, *No Assistance*) were significantly different in all participants (Table III). The means of *Average EMG* were not significantly different among *Movement*, however. No interaction effect was found between *Device* and *Movement*. The mean of *Average EMG* assisted by the *Utah Exo* was found to be significantly lower than when *No Assistance* was provided during post-hoc tests ($p = 0.0018$), as shown in Fig. 4A. Similarly, the medians of *Error* were significantly different among the three *Device* groups, regardless of the *Movement* types, in all participants (Table III). Significant differences exist in all pairwise comparisons, i.e. between *Columbia Exo* and *No Assistance* ($p = 0.006$), between *Utah Exo* and *No Assistance* ($p < 0.001$), and between *Columbia Exo* and *Utah Exo* ($p = 0.0028$).

When the visual feedback was removed, participants were instructed to relax and rely on the assistance from the exoskeleton for each movement. The means of *Average EMG* in all participants were found to be significantly different among *Device*, but not among *Movement*; no interaction effect was found between the two factors. This significant result was due to the significant differences found between assisted by either device and received *No Assistance* ($p = 0.0141$ for *Columbia Exo* and $p = 0.0001$ for *Utah Exo*, respectively), as shown in Fig. 4C. Additionally, among all participants, the medians of *Error* were found to be significantly different among *Device* groups in all types of *Movement* (Table III). As shown in Fig. 4D, when comparing *Error* assisted by the *Utah Exo* against either *Columbia Exo* or *No Assistance*, significant difference was found ($p < 0.001$ and $p = 0.0136$, respectively).

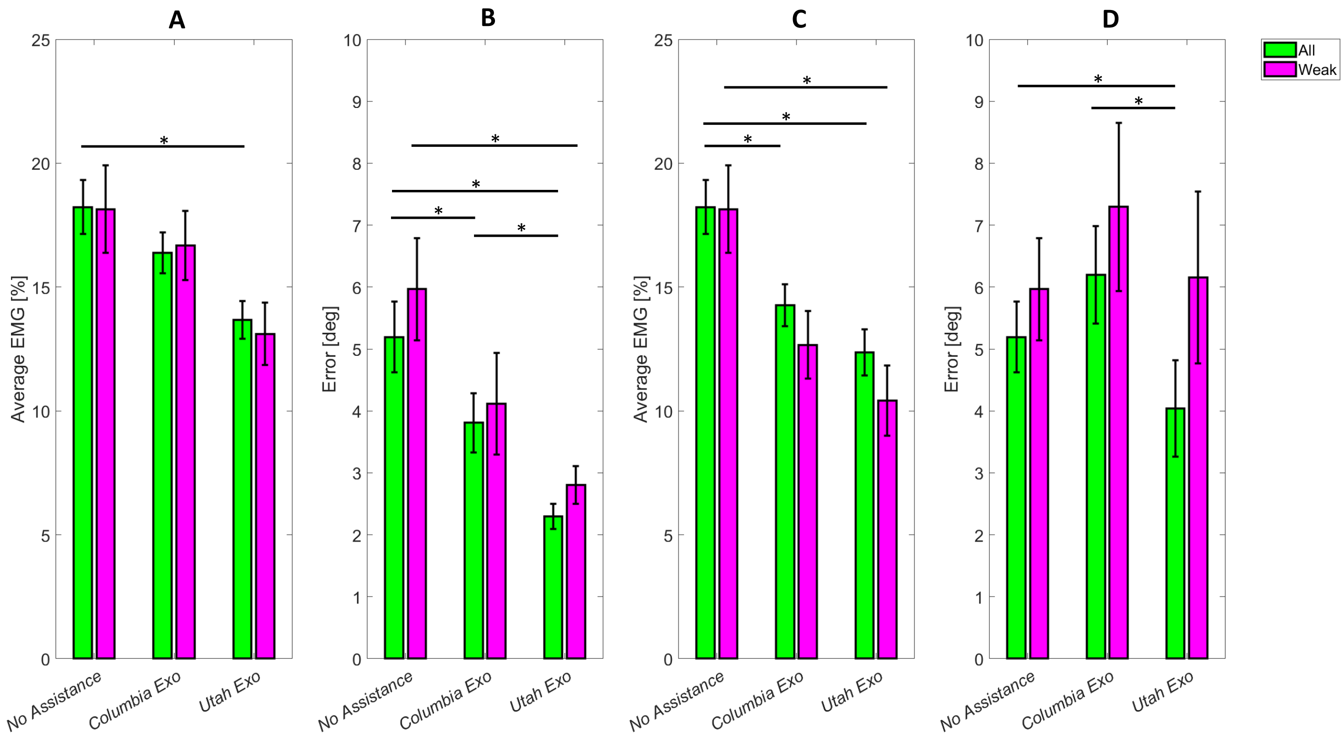

Fig. 4. **Comparison of response variables among *Device* groups between all participants and only participants with self-reported weakness, during Visual (A and B) and No Visual (C and D) conditions.** (A) *Average EMG* in all participants and in participants with self-reported weakness during Visual condition. (B) Tracking *Error* in all participants and in participants with self-reported weakness during Visual condition. (C) *Average EMG* in all participants and in participants with self-reported weakness during No Visual condition. (D) Tracking *Error* in all participants and in participants with self-reported weakness during No Visual condition. The bars indicate the group mean and the whiskers indicate the group standard error, respectively. The asterisks indicate the significant results.

Furthermore, when the data only included patients with self-reported weakness, the means of *Average EMG* in patients with weakness were found to be similar among three *Device* groups when the visual feedback was present, but became significantly different when the visual feedback was removed. The types of *Movement* did not contribute to the finding, and no interaction effect was found between *Movement* and *Device* factors. Post-hoc analysis (Fig. 4B) shows that the significance in No Visual condition was caused by difference in means of *Average EMG* between *No Assistance* and *Utah Exo* groups ($p = 0.0062$). By contrast, the medians of *Error* were found to be significantly different among the three *Device* groups when the visual feedback was provided. However, these differences were not significant when the visual feedback was removed and the participants were encouraged to rely on the robot assistance. Post-hoc comparisons (Fig. 4D) show that the significance in Visual condition was only contributed by comparing median of *Error* between *No Assistance* and *Utah Exo* groups ($p < 0.001$).

After concluding the evaluation with each exoskeleton, participants were asked 12 questions in the same order regarding their satisfaction with the respective exoskeleton. They provided their response to each question on a 7-point Likert scale (Table IV). Participants rated the two exoskeletons similarly for factors (Q3∼10) that we attempted to keep similar ($p > 0.05$). This means that any biomechanical results presented above were not caused by these factors (e.g., the greater reduction in neck muscle activation associated with the *Utah Exo* was not because it was more securely attached to the body). Furthermore, regardless of which exoskeleton they used, all participants (except one without any remaining hand functions) preferred to move their head to make eye contact during the simulated conversation using the joystick (Q12) and agreed that the joystick control was reasonably easy to use (Q11). While most participants commented that they felt the *Utah Exo* offered more support to their head during the experiment, we did not find significant difference between their ratings in terms of sufficiency of support (Q1) and alignment of the exoskeleton to their natural head-neck motions (Q2) ($p > 0.05$). Overall, participants responded positively regarding both neck exoskeletons. All participants rated in favor of the neck exoskeletons as compared to responding "Neutral" to the survey questions ($p < 0.001$). On average, participants rated 5.56 ± 0.16 and 5.65 ± 0.21 (Mean±Standard Error) for the *Columbia Exo* and the *Utah Exo*, respectively, among all questions.

IV. Discussion

Neck exoskeletons represent a viable alternative solution to not only support but also actively enable head-neck motions in ALS patients. To date, most neck exoskeletons use parallel mechanisms in their design to support the weight of the head and accommodate the large range, spatial rotations of the head [12], [13], [24], [25], [26], [27], [28]. This is because all actuators can be placed on the proximal joints and extra linkage chains provide additional support to counterbalance

TABLE IV
SURVEY QUESTIONS AND RESPONSES

	Columbia Exo mean rating (median), interquartile range	*Utah Exo* mean rating (median), interquartile range
Q1. I feel that this device offers sufficient support to my head.	6 (6), 2	5.33 (5.5), 2
Q2. I feel that the movement of this device aligned with my natural head movement.	4.5 (5), 1	5.33 (5.5), 1
Q3. I prefer this device to other devices (e.g., braces) that I have used.	6 (7), 2.25	6.67 (7), 0.75
Q4. I feel that this device is securely attached to my shoulders.	4.83 (5), 2	4 (4), 4
Q5. I feel that this device is securely attached to my head.	4.67 (4.5), 3	5.2 (5.5), 4
Q6. I feel that this device is comfortable to wear.	4 (4), 2	5 (5), 2
Q7. I feel that the weight of this device is acceptable.	6.17 (6), 1	6 (6), 0
Q8. I feel that this device is easy to put on.	5.2 (5), 1.25	5 (5), 2
Q9. I feel that this device does not hinder my ability to speak.	6.25 (7), 1.5	6.25 (7), 1.5
Q10. I feel that this device does not hinder my ability to breathe.	6.8 (7), 0.25	6.6 (7), 1
Q11. I feel that the joystick is easy to use.	6 (6), 1	6.25 (6), 0.5
Q12. I prefer to answer these questions with the joystick turned on.	6.25 (6.5), 1.5	6.25 (6), 0.5

Notes: 12 questions were asked to each participant after evaluating each exoskeleton. The questions were asked in the same order. We assigned numbers to the 7-point Likert scale as follows: Strongly Agree =7; Agree=6; Somewhat Agree=5; Neutral=4; Somewhat Disagree=3; Disagree=2; Strongly Disagree=1.

the weight of the head. As a result, the moving inertia is greatly reduced and smaller actuators can be used, which, in turn, allows for a smaller and lighter wearable robot. However, because the distal joints are not actuated, parallel mechanisms may be perturbed easily at certain configurations due to singularities and errors in fabrication to meet the kinematic constraints [29], [30], [31], [32]. These limitations cause insufficient transmission of the actuator power to the head attachment. i In the *Utah Exo*, we applied a weighted optimization to prioritize the structural stability over the range of motion. We focused on maximizing the structural stability by minimizing the condition number of the Jacobian matrix while achieving a reasonable exoskeleton workspace [18]. As an observation (Fig. 1A and B), a clear difference between the *Utah Exo* and the *Columbia Exo* is that the distal linkages in the *Utah Exo* are more angled and placed farther away from each other to connect to the head attachment. This creates larger moment arms and better maneuverability to move the head. In contrast, in the *Columbia Exo* the distal linkages are close together and two of the three links are also nearly vertical to support the head attachment at the upright pose. Considering that the mechanism is quasi-spherical, this arrangement is mechanically less advantageous to apply the moment on the head. In our bench experiments, we showed that the *Utah Exo* has an improved ability to resist external perturbations [18].

We postulated that the structural enhancements would translate to providing greater assistance for patients with ALS. Specifically, we expected that the neck muscle activation would be lower when following instructed motions (displayed on the screen) with assistance from the *Utah Exo*, as compared to the *Columbia Exo*. We also expected that when the participants completely relax and allow the exoskeletons to move their head, following prescribed motion, the *Utah Exo* would result in more accurate tracking than the *Columbia Exo*. Through our evaluation, we found that compared to receiving *No Assistance*, using the *Utah Exo* significantly reduced the EMG of neck muscles ($18.2 \pm 1.1\%$ v. $13.6 \pm 0.7\%$) while improving the tracking performance ($5.2 \pm 0.6°$ v. $2.2 \pm 0.2°$). Although *Columbia Exo* also helped improve tracking ($3.8 \pm 0.5°$), it did not significantly decrease the muscular effort input by the participants ($16.4 \pm 0.8\%$). Moreover, when completely relying on the exoskeleton assistance without visual feedback, the tracking performance was significantly improved when using the *Utah Exo* ($4.0 \pm 0.8°$). By contrast, the *Columbia Exo* worsened, albeit slightly, the tracking performance ($6.2 \pm 0.8°$). These results show that the enhanced structural stability in the *Utah Exo* indeed reduces the necessary muscle effort of the user to track the target head-neck trajectories while decreasing error in the target kinematics. Furthermore, we showed that the biomechanical benefits were retained in patients with self-reported weakness, as evidenced by the reduced EMG in neck muscles and improved tracking kinematics when assisted by the *Utah Exo* as compared to receiving *No Assistance* (Fig. 4). These results can be attributed to the stronger support offered by the *Utah Exo*, as the participants were better assisted through the target trajectories and they did not need to input much of their own muscular effort to stay on these prescribed trajectories. Our results also showed that the biomechanical benefits persisted across different movement tasks, suggesting that the structural stability of the neck exoskeleton consistently improved the user's ability to perform a wide range of head-neck movements.

Overall, participants were satisfied with the neck exoskeletons as they responded positively to all survey questions which were focused on comfort and usability of the devices. Participants responded similarly between the two exoskeletons, with no apparent preference towards either device. This result confirmed that participants were not biased towards one exoskeleton over another, which allowed us to draw a conclusion that the observed biomechanical benefits using the *Utah Exo* were primarily due to its superior structural stability. Additionally, as a demonstration for future clinical translation, we showed how patients could potentially benefit from the neck exoskeletons in their daily activities through a simulated conversation task. In contrast with the head being held upright, similar to wearing a static neck collar, all participants preferred to, without prompt, rotate their head and make eye contact during the conversation. These results highlight the importance of restoring head-neck mobility to improve the physical and emotional well-being of patients with ALS.

As patients with ALS are known to fatigue frequently, we designed the experiment to be under two hours through our protocol iteration process. Therefore, only a few movements were chosen in this experiment which are limited to sagittal and transverse planes. We also mitigated the issue of fatigue by randomizing the order of evaluating the devices among participants. Half of the participants started with the *Columbia Exo*, while the other half started with the *Utah Exo*. As a pilot study, the results presented in this paper may be limited by the number of participants. However, post-hoc power analysis suggests that some of our results may have been sufficiently powered. For example, when comparing *Average EMG* between assisted by the *Utah Exo* and receiving *No Assistance*, our result has a power of 0.99 (Cohen's d effect size $d = 4.86$). During the Baseline conditions, participants used the exoskeletons with the motors unpowered. We have previously shown that the *Columbia Exo* is very back-drivable when unpowered [23]. The observed EMG during Baseline sessions using the two devices were similar, which means the structural improvement in *Utah Exo* did not increase the effort to back drive the exoskeleton when the motors were unpowered. Therefore, we believe that participants did not overuse their muscles during the baselines. However, a true baseline measurement where only external sensors (e.g., IMUs, camera-based motion capture systems) are used may provide a more direct measurement of the head kinematics and neck muscle activation. Additionally, despite efforts to design joystick handles that are easy to grasp, one participant who had complete loss of hand/wrist functions could not use the joystick as the control input. This highlights the importance of designing new control interfaces in order to translate the neck exoskeletons to patients with ALS.

The present study mainly focused on laboratory-based tasks to evaluate the effects of exoskeleton structural stability on biomechanical performances in ALS users. Future work will extend evaluation of the Utah Neck Exoskeleton in other real-life tasks (e.g., look for traffic, clear a table, etc.) and other factors that are important for patient adoption (e.g., aesthetics, donning/doffing, sound, suitability in social settings, etc.). Additionally, lessons learned from the current study, such as necessity of hand-free control and potential need for wheelchair integration, will guide future development decisions of the neck exoskeleton. We believe these important steps will help lead to an eventual clinically available neck exoskeleton that will be suitable for patients with ALS to treat their dropped head condition, ultimately improving their quality of life.

V. Conclusion

This paper presents a study to evaluate the effect of the mechanical structure of a neck exoskeleton on head-neck movement assistance in patients with ALS. Our results suggested that the structural stability is an important factor to achieve desired biomechanical benefits (e.g., muscle activation and head kinematics). The structural improvement also allows the biomechanical benefit to be retained in participants with severe neck muscle weakness who are the intended users. Furthermore, we demonstrated that participants with ALS are generally satisfied with the neck exoskeleton technology and preferred to use the neck exoskeletons when possible to perform a simulated conversation task. These results highlighted the importance of structural design of neck exoskeletons for patients with ALS. As head-neck motions are essential in both functional and social tasks, this study demonstrated how a neck exoskeleton can potentially be used to improve the quality of life of patients with ALS.

Acknowledgment

The authors would like to thank the six participants with amyotrophic lateral sclerosis and their families for their time participating in this study and for their valuable feedback on the robotic systems. They also like to thank Dr. Summer Gibson for helping with the patient recruitment, Ian Bales and Kimia Khoshnami for their help with conducting the experiments, and Dr. Rosemaire Murray for her manuscript suggestions.

References

[1] M. Uemura et al., "Dropped head syndrome in amyotrophic lateral sclerosis," *Amyotrophic Lateral Sclerosis Frontotemporal Degeneration*, vol. 14, no. 3, pp. 232–233, Apr. 2013.

[2] L. P. Rowland and N. A. Shneider, "Amyotrophic lateral sclerosis," *New England J. Med.*, vol. 344, no. 22, pp. 1688–1700, 2001.

[3] S. Pinto and M. de Carvalho, "Dropped head presentation in ALS," *Amyotrophic Lateral Sclerosis Frontotemporal Degeneration*, vol. 14, no. 3, p. 235, Apr. 2013.

[4] T. P. Bleck, "Dropped head syndrome," *Neurology*, vol. 43, no. 4, p. 846, Apr. 1993.

[5] A. J. Waclawik, B. P. Lotz, B. R. Beinlich, and B. R. Brooks, "Dropped head syndrome," *Neurology*, vol. 48, no. 2, pp. 550–551, 1997.

[6] S. D. J. Spears, Y. F. Abdulle, D. Korovilas, R. Torii, D. M. Kalaskar, and N. Sharma, "Neck collar assessment for people living with motor neuron disease: Are current outcome measures suitable?" *Interact. J. Med. Res.*, vol. 12, Mar. 2023, Art. no. e43274.

[7] M. Gourie-Devi, A. Nalini, and S. Sandhya, "Early or late appearance of 'dropped head syndrome' in amyotrophic lateral sclerosis," *J. Neurol., Neurosurgery Psychiatry*, vol. 74, no. 5, pp. 683–686, 2003.

[8] A. L. Ward et al., "Power wheelchair prescription, utilization, satisfaction, and cost for patients with amyotrophic lateral sclerosis: Preliminary data for evidence-based guidelines," *Arch. Phys. Med. Rehabil.*, vol. 91, no. 2, pp. 268–272, Feb. 2010.

[9] H. Reed et al., "Head-up; An interdisciplinary, participatory and co-design process informing the development of a novel head and neck support for people living with progressive neck muscle weakness," *J. Med. Eng. Technol.*, vol. 39, no. 7, pp. 404–410, Oct. 2015.

[10] S. Baxter et al., "Evaluating a novel cervical orthosis, the Sheffield support snood, in patients with amyotrophic lateral sclerosis/motor neuron disease with neck weakness," *Amyotrophic Lateral Sclerosis Frontotemporal Degeneration*, vol. 17, nos. 5–6, pp. 436–442, Aug. 2016.

[11] S. Pancani, W. Tindale, P. J. Shaw, C. Mazza, and C. J. McDermott, "Efficacy of the head up collar in facilitating functional head movements in patients with amyotrophic lateral sclerosis," *Clin. Biomechanics*, vol. 57, pp. 114–120, Aug. 2018.

[12] H. Zhang and S. K. Agrawal, "An active neck brace controlled by a joystick to assist head motion," *IEEE Robot. Autom. Lett.*, vol. 3, no. 1, pp. 37–43, Jan. 2018.

[13] H. Zhang and S. K. Agrawal, "Kinematic design of a dynamic brace for measurement of head/neck motion," *IEEE Robot. Autom. Lett.*, vol. 2, no. 3, pp. 1428–1435, Jul. 2017.

[14] H. Zhang, B. Chang, J. Andrews, H. Mitsumoto, and S. Agrawal, "A robotic neck brace to characterize head-neck motion and muscle electromyography in subjects with amyotrophic lateral sclerosis," *Ann. Clin. Translational Neurol.*, vol. 6, no. 9, pp. 1671–1680, Sep. 2019.

[15] L. Z. F. Chiu, "Biomechanical methods to quantify muscle effort during resistance exercise," *J. Strength Conditioning Res.*, vol. 32, no. 2, pp. 502–513, 2018.

[16] T. Lenzi, S. M. M. De Rossi, N. Vitiello, and M. C. Carrozza, "Intention-based EMG control for powered exoskeletons," *IEEE Trans. Biomed. Eng.*, vol. 59, no. 8, pp. 2180–2190, Aug. 2012.

[17] H. Zhang, B.-C. Chang, P. Kulkarni, J. Andrews, N. A. Shneider, and S. Agrawal, "Amyotrophic lateral sclerosis patients regain head-neck control using a powered neck exoskeleton," in *Proc. 9th IEEE RAS/EMBS Int. Conf. Biomed. Robot. Biomechatronics (BioRob)*, Aug. 2022, pp. 01–06.

[18] D. Demaree and H. Zhang, "A structurally enhanced neck exoskeleton to assist with head-neck motion," in *Proc. Int. Symp. Med. Robot. (ISMR)*, Apr. 2023, pp. 1–7.

[19] H. Zhang, K. Albee, and S. K. Agrawal, “A spring-loaded compliant neck brace with adjustable supports,” *Mechanism Mach. Theory*, vol. 125, pp. 34–44, Jul. 2018.

[20] H. Zhang, “A novel robotic platform to assist, train, and study head-neck movement,” *ProQuest Diss. Theses*, p. 101, 2019. [Online]. Available: https://login.ezproxy.lib.utah.edu/login?url=https://www.proquest.com/dissertations-theses/novel-robotic-platform-assist-train-study-head/docview/2309521904/se-2

[21] J. Pusey, A. Fattah, S. Agrawal, and E. Messina, “Design and workspace analysis of a 6–6 cable-suspended parallel robot,” *Mechanism Mach. Theory*, vol. 39, no. 7, pp. 761–778, 2004.

[22] H. Zhang, B.-C. Chang, and S. K. Agrawal, “Using a robotic neck brace for movement training of the head–neck,” *IEEE Robot. Autom. Lett.*, vol. 4, no. 2, pp. 846–853, Apr. 2019.

[23] H. Zhang, B.-C. Chang, Y.-J. Rue, and S. K. Agrawal, “Using the motion of the head-neck as a joystick for orientation control,” *IEEE Trans. Neural Syst. Rehabil. Eng.*, vol. 27, no. 2, pp. 236–243, Feb. 2019.

[24] J. Liu, Y. Cheng, S. Zhang, Z. Lu, and G. Gao, “Design and analysis of a rigid-flexible parallel mechanism for a neck brace,” *Math. Problems Eng.*, vol. 2019, pp. 1–20, Nov. 2019, doi: 10.1155/2019/9014653.

[25] M. E.-H. Ibrahem, M. T. El-Wakad, M. S. El-Mohandes, and S. A. Sami, “Implementation and evaluation of a dynamic neck brace rehabilitation device prototype,” *J. Healthcare Eng.*, vol. 2022, pp. 1–12, Oct. 2022. [Online]. Available: https://www.ncbi.nlm.nih.gov/pmc/articles/PMC9633188/

[26] P. Lingampally and A. Selvakumar, “A kinematic and workspace analysis of a parallel rehabilitation device for head-neck injured patients,” *FME Trans.*, vol. 47, no. 3, pp. 405–411, 2019.

[27] A. Lozano, M. Ballesteros, D. Cruz-Ortiz, and I. Chairez, “Active neck orthosis for musculoskeletal cervical disorders rehabilitation using a parallel mini-robotic device,” *Control Eng. Pract.*, vol. 128, Nov. 2022, Art. no. 105312.

[28] V. E. Abarca and D. A. Elias, “A review of parallel robots: Rehabilitation, assistance, and humanoid applications for neck, shoulder, wrist, hip, and ankle joints,” *Robotics*, vol. 12, no. 5, p. 131, Sep. 2023. [Online]. Available: https://www.mdpi.com/2218-6581/12/5/131

[29] I. A. Bonev and C. M. Gosselin, “Singularity loci of spherical parallel mechanisms,” in *Proc. IEEE Int. Conf. Robot. Autom.*, Apr. 2005, pp. 2957–2962.

[30] D. Zlatanov, I. A. Bonev, and C. M. Gosselin, “Constraint singularities of parallel mechanisms,” in *Proc. IEEE Int. Conf. Robot. Autom.*, May 2002, pp. 496–502.

[31] J. T. Wen and J. F. O’Brien, “Singularities in three-legged platform-type parallel mechanisms,” *IEEE Trans. Robot. Autom.*, vol. 19, no. 4, pp. 720–726, Aug. 2003.

[32] D. Zlatanov, R. G. Fenton, and B. Benhabib, “Singularity analysis of mechanisms and robots via a motion-space model of the instantaneous kinematics,” in *Proc. IEEE Int. Conf. Robot. Autom.*, May 1994, pp. 980–985.